



저작자표시-비영리-변경금지 2.0 대한민국

이용자는 아래의 조건을 따르는 경우에 한하여 자유롭게

- 이 저작물을 복제, 배포, 전송, 전시, 공연 및 방송할 수 있습니다.

다음과 같은 조건을 따라야 합니다:



저작자표시. 귀하는 원저작자를 표시하여야 합니다.



비영리. 귀하는 이 저작물을 영리 목적으로 이용할 수 없습니다.



변경금지. 귀하는 이 저작물을 개작, 변형 또는 가공할 수 없습니다.

- 귀하는, 이 저작물의 재이용이나 배포의 경우, 이 저작물에 적용된 이용허락조건을 명확하게 나타내어야 합니다.
- 저작권자로부터 별도의 허가를 받으면 이러한 조건들은 적용되지 않습니다.

저작권법에 따른 이용자의 권리는 위의 내용에 의하여 영향을 받지 않습니다.

이것은 [이용허락규약\(Legal Code\)](#)을 이해하기 쉽게 요약한 것입니다.

[Disclaimer](#)

Thesis for the Degree of Master of Landscape Architecture

**Modeling Carbon and Energy Fluxes
in a Heterogeneous Urban Park**

이질적 도시 공원에서의 탄소와 에너지 플럭스 모델링

February, 2015

Graduate School of

Seoul National University

Department of Landscape Architecture and Rural Systems

Engineering, Landscape Architecture Major

Kimm, Hyungsuk

Modeling Carbon and Energy Fluxes in a Heterogeneous Urban Park

이질적 도시 공원에서의 탄소와 에너지 플럭스 모델링

Under the Direction of Adviser, **Prof. Ryu, Youngryel**

Submitted to the Faculty of
the Graduate School of Seoul National University
December, 2014

By **Kimm, Hyungsuk**

The Graduate School of Seoul National University
Department of Landscape Architecture and Rural Systems
Engineering, Landscape Architecture Major

Approved as a Qualified Thesis of Kim, Hyungsuk
for the Degree of Master of Landscape Architecture
by the Committee
January, 2015

CHAIRMAN _____

VICE CHIARMAN _____

MEMBER _____

Abstract

Parks account for a large proportion of green spaces in urban regions, but most previous studies have focused on the values of recreational services in urban parks—carbon uptake by plants in urban parks has been studied less extensively. Urban parks typically form complex landscapes in space and time by integrating multiple species with open canopies. Thus, to better understand canopy photosynthesis in urban park, measuring spatial and temporal variations in photosynthetic parameters and canopy structural variables is essential. Here, we report seasonal and spatial variations in two key photosynthetic parameters (V_{cmax} and J_{max} which are the maximum rates of carboxylation and electron transport, respectively) and leaf area index (LAI) in Seoul Forest Park. During the peak growing season, we found an eightfold difference (20 to 149 $\mu\text{mol m}^{-2} \text{s}^{-1}$) and fourfold difference (38 to 141 $\mu\text{mol m}^{-2} \text{s}^{-1}$) in V_{cmax} and J_{max} , respectively, across 10 species. Over the seasons, two woody species (*Zelkova serrata* and *Prunus yedoensis* Matsum) respectively showed three- to fivefold differences in V_{cmax} and two- to fivefold differences in J_{max} . We evaluated whether leaf nitrogen contents could predict V_{cmax} and J_{max} , and found significant correlations among the three variables during the peak growing season across 10 species, but no significant correlations among them over the seasons in the two woody

species. LAI computed using in- situ observations and satellite remote-sensing imagery showed a non-normal distribution with marked variation during the growing season. A sophisticated 3 dimensional model, which reflects complexity of vegetation structure in the park, well predicted carbon and energy fluxes for a day. Moreover, the model simulation with simplistic virtual scenarios clearly showed the effects of difference in tree distribution and tree size on carbon and energy fluxes (~ 3 % and ~ 40 %, respectively). These results highlight not only necessity of consideration of spatial and temporal variability in photosynthetic parameters and LAI for accurate estimation of canopy photosynthesis in urban parks, but also an important role of individual tree based model as a potential park design evaluating platform.

Keywords: leaf area index, maximum rate of carboxylation, maximum rate of electron transport, photosynthesis, 3D modeling, urban park

Student Number: 2013-21147

CONTENTS

ABSTRACT	i
CONTENTS	iii
LIST OF TABLES	v
LIST OF FIGURES	v
I. INTRODUCTION	1
II. MATERIALS AND METHODS	6
1. Site	6
2. Photosynthetic parameters and leaf traits measurement	6
3. Leaf area index measurement	8
3.1. Plot design	8
3.2. Digital cover photography	10
4. Satellite remote-sensing data processing	12
5. Model simulation	13
5.1. Model description	13
5.2. Collecting crown data	13
5.3. Flux measurement	14
5.4. Simulations with virtual scenarios	14
III. RESULT AND DISCUSSION	16
1. To what extent do photosynthetic parameters vary spatially during the peak growing season and temporally across the seasons? ...	16

2. Can V_{cmax} and J_{max} be estimated indirectly from leaf traits data?	20
3. To what extent does the LAI vary across different land cover types over the seasons?	24
4. Can park design strategy affect carbon and energy fluxes?	27
5. Broader implications for future urban park design	30
 IV. SUMMARY AND CONCLUSIONS	 32
 REFERENCE	 34
ABSTRACT (<i>Korean</i>)	42
ACKNOWLEDGEMENT	44

LIST OF TABLES

Table 1. Species composition in each plot

Table 2. Description of scenarios for model simulation. LAD, LAI, CC represents leaf area density (m^2/m^3), leaf area index (m^2/m^2), crown cover (%), respectively. “ELEMENTS” shows the profile of individual trees in scenarios.

LIST OF FIGURES

Figure 1. (a) V_{cmax} and (b) J_{max} in 10 species measured during the peak growing season. Error bars indicates 95% CI.

Figure 2. Seasonal variation in (a) V_{cmax} and (b) J_{max} for *Zelkova serrata* and *Prunus yedoensis Matsum.* Error bars indicate 95% CI.

Figure 3. Comparison of the leaf nitrogen content per unit area and V_{cmax} for 10 species measured during the peak growing season.

Figure 4. Comparison of V_{cmax} and J_{max} for 10 species measured during the peak growing season.

Figure 5. Seasonal trend in leaf nitrogen content per unit area for *Zelkova serrata* and *Prunus yedoensis Matsum.* Error bars indicate 95% CI. The shaded area represents the monsoon period.

Figure 6. Seasonal variation in the leaf area index in 10 plots.

Figure 7. (a) Leaf area index (LAI) map for day of year (DOY) 259 derived from Landsat images. (b) Histograms of Landsat-derived LAI values in the park for DOY 86, 131, 179, 259, and 355. The curves

indicate histograms fit to a normal distribution.

Figure 8. Satellite image (left), and visualized input data (right) of the model simulation plot site (120 m by 120 m). Circles in both plots represents the footprint of the eddy covariance measurement.

Figure 9. Comparison between the simulated- , and measured carbon and energy fluxes in the plot.

Figure 10. Difference of results between SCN_1 and SCN_2, and SCN_1 and SCN_3.

Figure 11. Difference of results between SCN_L and SCN_M, SCN_L and SCN_MX, and SCN_L and SCN_S.

I. INTRODUCTION

The number of urban parks is expected to increase in many urban regions due to rapid urbanization (Angel et al., 2011; Seto and Fragkias, 2005; Seto et al., 2012) and citizens' desire for a better quality of life (Chiesura, 2004; Jim and Chen, 2006; Thompson, 2002). As urban parks account for a large proportion of green spaces in urban regions, they might partially offset carbon dioxide (CO₂) emissions in urban regions which are responsible for more than 60% of global CO₂ emissions (Biol et al., 2008; IEA, 2013). Although a few studies have attempted to quantify carbon (C) stocks in vegetation and soils in urban parks (Bae and Ryu, 2014; Huttyra et al., 2011), to our knowledge, none has quantified canopy photosynthesis, the main driver of the C cycle (Beer et al., 2010; Ryu et al., 2011).

To quantify canopy photosynthesis, an understanding of leaf-level photosynthesis is essential. The Farquhar–von Caemmerer–Berry (FvCB) model proposed a mechanistic photosynthesis paradigm (Farquhar et al., 1980), which has been widely used in predicting photosynthesis from the leaf, to global scales (dePury and Farquhar, 1997; Ryu et al., 2011; Sellers et al., 1997). The FvCB model adopts a biochemical approach based on the mechanism of the Calvin cycle, which is limited by the carboxylation rate [i.e., the amount of activated photosynthesis enzyme ribulose-1,5-

bisphosphate carboxylase/oxygenase (Rubisco)], or electron transport rate [i.e., regeneration rate of the substrate of Rubisco, ribulose bisphosphate (RuBP)]. The model computes photosynthesis separately under two assumptions: that the Calvin cycle is limited by the rate of either carboxylation or electron transport. Finally, the model provides the minimum value of the two as a photosynthesis rate. Thus, the maximum carboxylation rate (V_{cmax}) and the maximum electron transport rate (J_{max}) are the key parameters in the FvCB model and are estimated based on CO_2 assimilation to leaf internal CO_2 concentration curve derived from leaf gas exchange measurements (Sharkey et al., 2007). Field observations revealed that both V_{cmax} and J_{max} varied with the environment as well as season (Muraoka et al., 2010; Wang et al., 2008; Wilson et al., 2000).

Indirect estimation of the photosynthetic parameters through positive correlations between leaf nitrogen (N) contents and V_{cmax} (Amthor, 1994; Friend, 1995), and between V_{cmax} and J_{max} (Wullschleger, 1993), would require less time and effort than direct estimation from leaf gas exchange measurements. Specifically, previous studies found a positive correlation between V_{cmax} and N content per leaf area (Kattge et al., 2009). This correlation is supported by the fact that V_{cmax} is affected by the amount of the N-rich enzyme Rubisco. Also, V_{cmax} and J_{max} were found to be positively correlated. Thompson et al (1992) suggested that plants maintain a balance

between V_{cmax} and J_{max} by optimizing the allocation of resources (i.e., N) between Rubisco and chlorophyll to maximize photosynthesis (Wilson et al., 2000; Wullschleger, 1993). Moreover, advanced studies investigated other relationships among various leaf traits, which included leaf N concentration, leaf dry mass per leaf area (LMA), leaf N content per area, V_{cmax} , J_{max} , and the maximum rate of photosynthesis (Osnas et al., 2013; Reich et al., 1991; Wilson et al., 2000; Wright et al., 2004). These relationships, however, have not been tested in urban parks.

The leaf area index (LAI), defined as the hemi-surface leaf area per unit ground area, is the key variable to scale up photosynthesis from leaves to canopies (Baldocchi, 1997; dePury and Farquhar, 1997; Leuning et al., 1995; Ryu et al., 2011). The LAI determines mainly light interception by leaves in a canopy, which initiates canopy photosynthesis. The LAI has been measured in several forest, grassland, and cropland ecosystems (Chen, 1996; Gower and Norman, 1991; Ryu et al., 2010c). Additionally, global satellite observation systems such as the NASA Terra and Aqua satellites, have provided LAI maps over the globe at a 1-km resolution, 8-day interval (Myneni et al., 2002). However, there have been few studies that measured LAI in urban parks. Furthermore, global satellite LAI products provide 1-5-km-resolution maps, and thus the LAI in most parks, with the exception of very large parks such as Central Park in Manhattan, are unlikely to be captured by global satellite

LAI products. Thus, our understanding of spatial and temporal variations in the LAI in urban parks is limited.

Quantifying the photosynthetic parameters V_{cmax} and J_{max} , and the LAI in urban park, is challenging due to the heterogeneity of canopy structures. To meet citizens' diverse needs, urban parks are composed of multiple species and are spatially heterogeneous with a complex composition of land cover, such as forests, ponds, playgrounds, and lawns (Bae and Ryu, 2014; Cao et al., 2010; Jim and Chen, 2006). Heterogeneous land cover result in an uneven distribution of vegetation and makes measuring the LAI of an urban park difficult (Millward and Sabir, 2010). Moreover, a complex species composition would impose difficulties in measuring photosynthetic parameters because of species-specific differences in photosynthetic parameters (Kattge et al., 2009; Medlyn et al., 1999). Moreover, urban park vegetation is also temporally heterogeneous. The phenological patterns of factors such as the timing of leaf-out and leaf-off might vary among species and crowns (Reich et al., 1991; Wilson et al., 2000).

This study aimed to quantify the spatiotemporal heterogeneity of photosynthetic parameters and the LAI in an urban park, Seoul Forest Park, and to evaluate 3D canopy photosynthesis model against measured flux data, eventually to simulate carbon flux in various scenarios. We estimated V_{cmax} and J_{max} for 10 representative species during a peak growing season. For two

common species in the park, *Zelkova serrata* and *Prunus yedoensis* Matsum, we estimated V_{cmax} and J_{max} across the seasons. We also measured the LAI in 10 plots over the seasons, which were combined with Landsat satellite imagery to produce spatial and temporal maps of LAI in the park. Model simulation has been conducted for a 120 m by 120 m plot by using manually measured tree profile data. Our scientific questions were as follows: 1) To what extent do photosynthetic parameters vary spatially during the peak growing season and temporally across the seasons? 2) Can V_{cmax} and J_{max} be estimated indirectly from leaf traits data? 3) To what extent does the LAI vary across different land cover types over the seasons? 4) Can park design strategy affect carbon and energy fluxes?

II. MATERIALS AND METHODS

1. Study site

The study site is an urban park, Seoul Forest Park, in Seoul, South Korea (37.544 N, 127.038 E). The park is located beside the Han River and covers an area of 1 km². The site experiences a temperate monsoon climate. The mean annual temperature is 12.5°C, and the mean annual precipitation is 1450 mm year⁻¹ (Korea Meteorological Administration). In 2013, the park contained over 415,000 woody plants of 95 species (Seoul Metropolitan Government).

2. Photosynthetic parameters and leaf traits measurement

To quantify the spatial and temporal variations in leaf traits, including V_{cmax} , J_{max} , LMA, and C and N concentrations, we selected 10 dominant species. Two species (*Z. serrata* and *Pr. yedoensis*) were used to estimate seasonal variations in leaf traits and eight species (*Ulmus parvifolia jacq*, *Quercus acutissima*, *Quercus palustris*, *Betula platyphylla*, *Ginkgo biloba*, *Celtis sinensis*, *Pinus densiflora*, and *Euonymus alatus*) were selected to quantify spatial variations of the leaf traits during the peak growing season (day of year, DOY 219–255). Because canopy photosynthesis models require sunlit leaf traits as input parameters, we sampled only sunlit leaves located at the

top of crowns or the outer side of the south face of isolated crowns (dePury and Farquhar, 1997; Kattge et al., 2009; Ryu et al., 2011). To sample sunlit leaves, we used 3-m-long pruning scissors. We chose one tree per one species and collected three branches each of which held at least three leaves. One leaf of each branch was used for leaf gas exchange measurements and all three leaves of the branch were transported to the laboratory for measurement of LMA, and leaf N and C concentrations.

We estimated the key photosynthetic parameters, V_{cmax} and J_{max} , from leaf gas exchange measurements using a portable photosynthesis system (Li-6400; Li-Cor Inc., Lincoln, NE, USA). First, we measured the photosynthesis rate (A) responding to leaf internal CO_2 concentrations (C_i) to obtain A/C_i curves. For each leaf, we used the automated program mode in Li-6400 to create a A/C_i curve by changing leaf external CO_2 concentrations (400, 200, 50, 100, 200 ... 1400 ppm). Second, we estimated V_{cmax} and J_{max} from the obtained A/C_i curves using a least-squares curve-fitting method to fit the measured A/C_i curve to the FvCB model. We estimated V_{cmax} and J_{max} using the Microsoft ExcelTM spreadsheet provided by Sharkey et al. (2007). We report V_{cmax} and J_{max} values that were corrected to the leaf temperature at 25°C.

To quantify LMA and foliar C and N concentrations, we scanned all sampled leaves and computed leaf areas using the MATLAB image-processing toolbox (MathWorks Inc., Woburn, MA, USA). Then we

measured the dry mass of each leaf using a high-precision scale (accuracy: 0.001 g, CUX220H; CAS Corp., Seoul, South Korea) after 48 h of oven-dry at 80.0°C (C-DH; Chang Shin Scientific Co., Pusan, South Korea). Dried leaves were ground into powder to estimate C and N concentrations using an Elemental Carbon Analyzer (Flash EA 1112; Thermo Electron Co., Waltham, MA, USA) at the National Instrumentation Center for Environmental Management (NICEM) of Seoul National University.

3. Leaf area index measurement

3.1. Plot design

We randomly established 10 20 × 20-m plots in the planted areas in the park. Ten plots represented one evergreen needleleaf forest (ENF), one mixed forest (MF), one deciduous needleleaf forest (DNF), and seven deciduous broadleaf forests (DBFs). The plots showed a tenfold difference in stem density and twofold difference in tree height. The stem density, mean tree height, and species composition of each plot are shown in Table 1.

Table 1. Species composition in each plot

Plots	STEM DENSITY (stem/m ²)	TREE HEIGHT (m)	SPECIES
DBF1	0.09	8	<i>Acer palmatum</i> Thumb, <i>Quercus mongolica</i>
DBF2	0.13	9	<i>Quercus acutissima</i> , <i>Acer</i> <i>Buegerianum</i>
DBF3	0.07	15	<i>Platanus acerifolia</i>
DBF4	0.12	11	<i>Quercus acutissima</i> , <i>Ginkgo biloba</i> , <i>Acer buegerianum</i> , <i>Aesculus turbinata</i>
DBF5	0.12	8	<i>Quercus acutissima</i> , <i>Prunus yedoensis</i> <i>Matsum</i> , <i>Zelkova serrata</i> , <i>Ulmus</i> <i>parvifolia jacq</i>
DBF6	0.04	8	<i>Zelkova serrata</i> , <i>Carpinus laxiflora</i> , <i>Acer palmatum</i>
DBF7	0.04	9	<i>Zelkova serrata</i>
DNF	0.39	11	<i>Ginkgo biloba</i>
MF	0.05	11	<i>Pinus strobus</i> , <i>Ulmus parvifolia jacq</i> , <i>Metasequoia glyptostroboides</i> , <i>Liriodendron tulipifera</i>
ENF	0.08	14	<i>Pinus densiflora</i>

3.2. Digital cover photography (DCP)

We used DCP to estimate the LAI (Macfarlane et al., 2007; Ryu et al., 2014; Ryu et al., 2012). Photographs were obtained at 1-m height under canopies using a digital single-lens reflex camera (Nikon 600D; Nikon, Tokyo, Japan). We obtained three to seven photographs per plot viewing toward 57° from the zenith direction. G-function is the projection coefficient of unit foliage area on a plane perpendicular to the view direction and at a 57° -view zenith angle; the G-function is 0.5 regardless of leaf inclination angle distributions (Nilson, 1971; Wilson, 1960). We chose the 57° -view zenith angle because measuring leaf inclination angles from the canopy top to bottom for various species was difficult. The lens had focal length of 28.8 mm (35-mm equivalent). We obtained photographs under the aperture priority mode and low aperture value ($>f/1/5.6$) to broaden the depth of field within photographs (Pentland, 1987). We also set the shutter speed to shorter than 1/15 s to avoid blurred photographs. We chose the proper exposure level manually by checking the histogram of the blue channel using a built-in camera liquid-crystal display (LCD) to minimize overexposed canopy pixels for accurate estimation of the LAI. Each time we visited the field, we obtained photographs at the same positions and in the same directions to minimize uncertainties caused by inconsistent sampling footprints. We obtained photographs every 2 weeks on average from DOY 121 to DOY 333.

To estimate the LAI from photographs, we first extracted the blue channel, which shows the most marked contrast between the sky and vegetation. In the blue channel histogram, we separated pixels into sky pixels or vegetation pixels using a two-corner method to set the thresholds for pixel classification (Macfarlane, 2011). The obtained binary images enabled us to calculate the fraction of crown cover (CC) and gap fraction within crowns; i.e., crown porosity (CP; Macfarlane et al., 2007) . Thus, we finally calculated the LAI using the modified Beer’s law (Ryu et al., 2012):

$$LAI = \frac{-CC \times \log(CP)}{k} \gamma , \quad (2)$$

where k is the light extinction coefficient [$G(57^\circ)/\cos(57^\circ)$] and γ is the needle-to-shoot area ratio. We computed the LAI for individual photographs then averaged the LAI values in one plot to account for foliar clumping effects (Ryu et al., 2010b). In the case of needleleaf species (*P. densiflora* and *Pinus strobus*), we measured the needle-to-shoot area ratio to account for foliar clumping effects appearing at the shoot scale as proposed by Ryu et al. (2014). The γ value for *P. densiflora* was 2.11 ± 0.28 . The image analysis was conducted with a technical computing language, MATLAB (MathWorks Inc.).

4. Satellite remote-sensing data processing

We used Landsat 8 imagery (30-m resolution). We selected satellite data for 5 days (DOY 86, 131, 179, 259, and 355) that had less than 10% cloud cover per image. To remove path radiance effects in the atmosphere, we adopted the dark object subtraction method (Song et al., 2001). To obtain corrected digital numbers after the atmospheric correction, we converted the digital numbers to spectral reflectance using conversion coefficients provided by the Landsat 8 metafile. We computed the normalized difference vegetation index (NDVI) using red and near-infrared reflectance (Tucker, 1979):

$$NDVI = \frac{\rho_{NIR} - \rho_{RED}}{\rho_{NIR} + \rho_{RED}}, \quad (3)$$

where ρ_{NIR} and ρ_{RED} are the spectral reflectance of near-infrared and red, respectively. We extracted NDVI values within each LAI measurement plot. To infer the LAI from the NDVI (Ryu et al., 2010a), we developed an exponential regression model ($LAI = 3.44 \exp(NDVI) - 3.38$; $R^2 = 0.79$, $P < 0.001$). Using this equation, we generated LAI maps from Landsat NDVI imagery for 5 days (DOY 86, 131, 179, 259, and 355).

5. Model simulation

We used FLiES combined with CANOAK to simulate carbon and energy fluxes based on 3D radiative transfer simulation. We collected tree position and profile data to construct individual trees in model simulation. Only DOY 153 has been chosen because it was the clearest day (i.e., clear sine curve in incoming shortwave radiation) with stable wind condition (the smallest footprint of the flux measurements) during the summer season in 2013.

5.1. Model description

A 3D radiative transfer model, FLiES simulated radiative transfer by a Monte Carlo ray tracing which is randomly simulating the path length of each of the 22.5 million photons based on probability of a scattering event. Simulated amounts of absorbed photons at three different range of wavelength, photosynthetically active radiation, near infrared, thermal infrared, were used to simulate photosynthesis, evapotranspiration, and skin temperature at different surfaces.

5.2. Collecting crown data

We measured tree size and position data through a series of field work. Positions of trees, tree height, crown depth, crown width, and diameter at breast height (DBH) have been measured within a 120 m by 120 m size plot.

We used typical tapes to measure DBH and crown width. For crown width measurement, we measured distance from a trunk to the end of the crown at four directions (0, 90, 180, 270), and then averaged 4 values. To obtain vertical size of trees, we used a laser meter (Leica DISTO™ D5, Leica Geosystems, Hexagon, Sweden) at distant location from target trees to measure distance and angles toward at specific points of trees. Through a simple calculation, we estimated tree height and crown depth. Tree positions were captured by using distances from two reference points.

5.3. Flux measurement

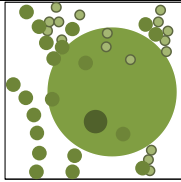
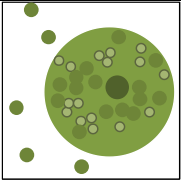
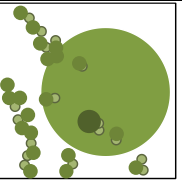
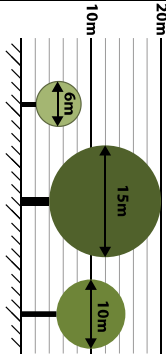
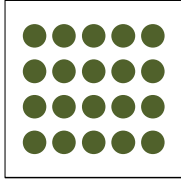
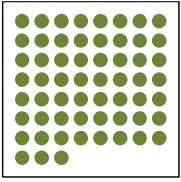
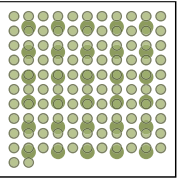
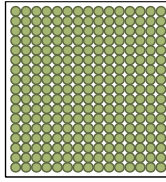
We measured carbon and water fluxes, and meteorological variables (air temperature, humidity, wind speed and direction, incoming shortwave radiation) with the Eddy covariance measurements on the top of a building in the park. We obtained 30 min averaged data of incoming shortwave radiation, wind speed and direction, carbon and water fluxes, air temperature, and humidity.

5.4. Simulations with virtual scenarios

We developed two sets of scenarios with difference in tree size and tree distribution. With the same set of trees, three scenarios, SCN_1, SCN_2, SCN_3, are composed with different tree distributions. In case of scenarios

with different tree sizes (SCN_L, SCN_M, SCN_MX, SCN_S), we adopted regular distributions of trees to only test the effect of different tree sizes with the same leaf area density and leaf area. Individual tree elements and the compositions are presented in Table 2.

Table 2. Description of scenarios for model simulation. LAD, LAI, CC represents leaf area density (m^2/m^3), leaf area index (m^2/m^2), crown cover (%), respectively. “ELEMENTS” shows the profile of individual trees in scenarios.

NAME	SCN_1	SCN_2	SCN_3	ELEMENTS
IMAGE				
LAD	1.623	1.623	1.623	
LAI	1.51	1.49	1.46	
CC	55.77	47.20	54.15	
NAME	SCN_L	SCN_M	SCN_MX	SCN_S
IMAGE				
LAD	1.623	1.623	1.623	1.623
LAI	2.95	2.92	2.91	2.99
CC	21.39	32.19	37.50	53.43

III. RESULTS AND DISCUSSION

1. To what extent do photosynthetic parameters vary spatially during the peak growing season and temporally across the seasons?

Two photosynthetic parameters, V_{cmax} and J_{max} , of the 10 species in the park presented a wide range of variation during the peak growing season [7.5-fold variation (from 20 to 149 $\mu\text{mol m}^{-2} \text{s}^{-1}$) in V_{cmax} and 3.7-fold variation (from 38 to 141 $\mu\text{mol m}^{-2} \text{s}^{-1}$) in J_{max} ; Fig. 1]. *Ulmus parvifolia jacq* and *C. sinensis* showed the highest and lowest V_{cmax} values (149 and 20 $\mu\text{mol m}^{-2} \text{s}^{-1}$, respectively), *E. alatus* and *C. sinensis* displayed the highest and lowest J_{max} values (141 and 38 $\mu\text{mol m}^{-2} \text{s}^{-1}$, respectively), and *U. davidiana* and *C. sinensis* had the highest and lowest values in the photosynthetic parameters. However, we observed that the species pairs were co-located within a 5-m distance in several places. In a meta-analysis study, Kattge et al. (2009) reported $57.7 \pm 21.2 \mu\text{mol m}^{-2} \text{s}^{-1}$ [mean \pm 1 standard deviation (S.D.), $n = 404$] V_{cmax} in temperate broad-leaved deciduous trees globally, while our results indicated $82.9 \pm 37.3 \mu\text{mol m}^{-2} \text{s}^{-1}$ in V_{cmax} ($n = 7$) for the same plant functional type trees, indicating greater variation in V_{cmax} .

The photosynthetic parameters of *Z. serrata* and *Pr. yedoensis* showed large seasonal variations (Fig. 2). Over the seasons, V_{cmax} varied from 20 to 100

$\mu\text{mol m}^{-2} \text{s}^{-1}$ and 40 to 120 $\mu\text{mol m}^{-2} \text{s}^{-1}$ for *Z. serrata* and *Pr. yedoensis*,

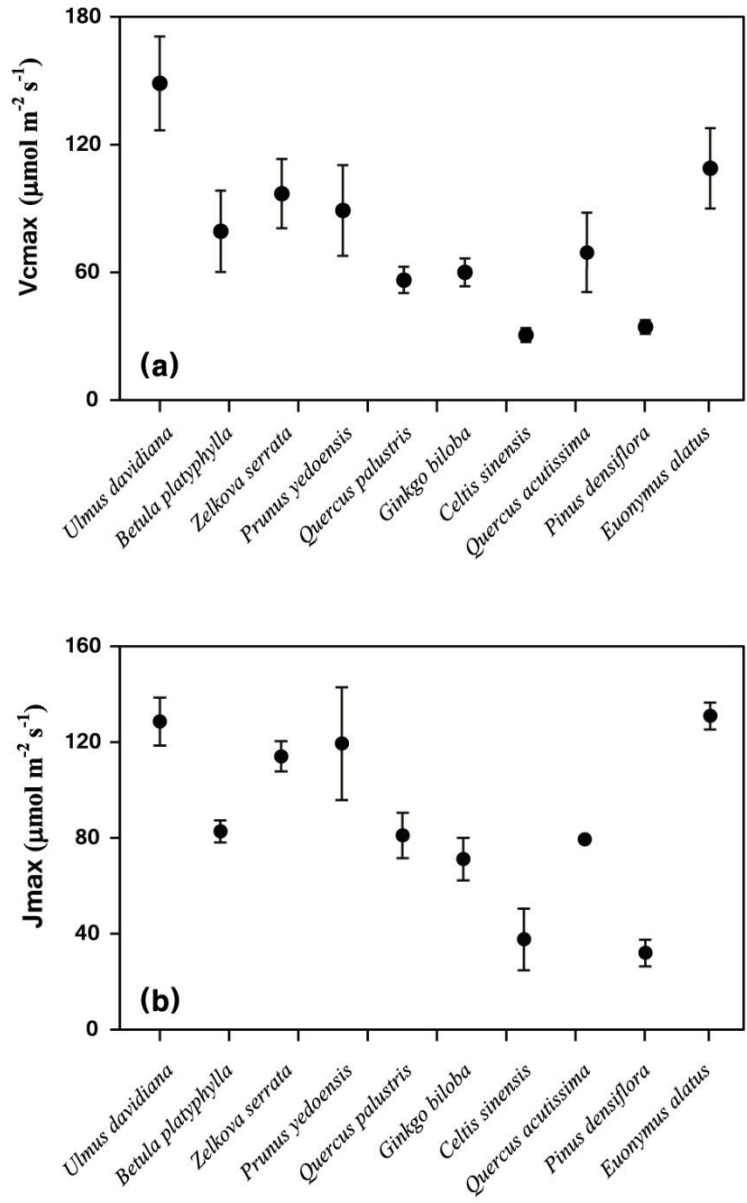


Fig. 1. (a) V_{cmax} and (b) J_{max} in 10 species measured during the peak growing season. Error bars indicates 95% CI.

respectively. The trends depicted leaf ontogeny and senescence, as reported for deciduous broad-leaved trees in previous studies (Muraoka et al., 2010; Wang et al., 2008; Wilson et al., 2000). Our results showed prolonged peak V_{cmax} values until DOY 250, followed by a reduction, which is similar to the findings of a study conducted in a temperate deciduous forest in Japan (Muraoka et al 2010).

The heterogeneous composition of plant species in urban parks, which caused marked variations in photosynthetic parameters, requires a different approach to canopy photosynthesis modeling. In natural ecosystems, high biodiversity of woody plants under an open canopy, which is the case in urban parks, is uncommon. For example, savanna is a typical case of open canopy but includes lower woody plant biodiversity, which are distributed sparsely (Baldocchi et al., 2004). In contrast, tropical forests have high woody plant biodiversity, which represent a closed canopy (Asner et al 2009). The large variation in V_{cmax} during the peak growing season in the urban park (20–149 $\mu\text{mol m}^{-2} \text{s}^{-1}$, nine species of woody plants) was greater than that reported previously in an Amazon tropical forest (30–80 $\mu\text{mol m}^{-2} \text{s}^{-1}$, 12 species; Domingues et al., 2012), a temperate deciduous forest (40–60 $\mu\text{mol m}^{-2} \text{s}^{-1}$, 4 species; Wilson et al 2000), and an woody savanna forest (130 $\mu\text{mol m}^{-2} \text{s}^{-1}$, 1 species; Baldocchi et al., 2004). Therefore, we assume that an individual-tree-based three-dimensional (3D) canopy photosynthesis model is more appropriate for estimating canopy photosynthesis in urban parks.

Conventional photosynthesis models—such as a big-leaf model (Sellers 1985) or two-leaf models (dePury and Farquhar 1997, Ryu et al 2011))—which simplify ecosystem structure and functions into one or two big leaves, are unlikely to simulate accurately canopy photosynthesis in urban parks.

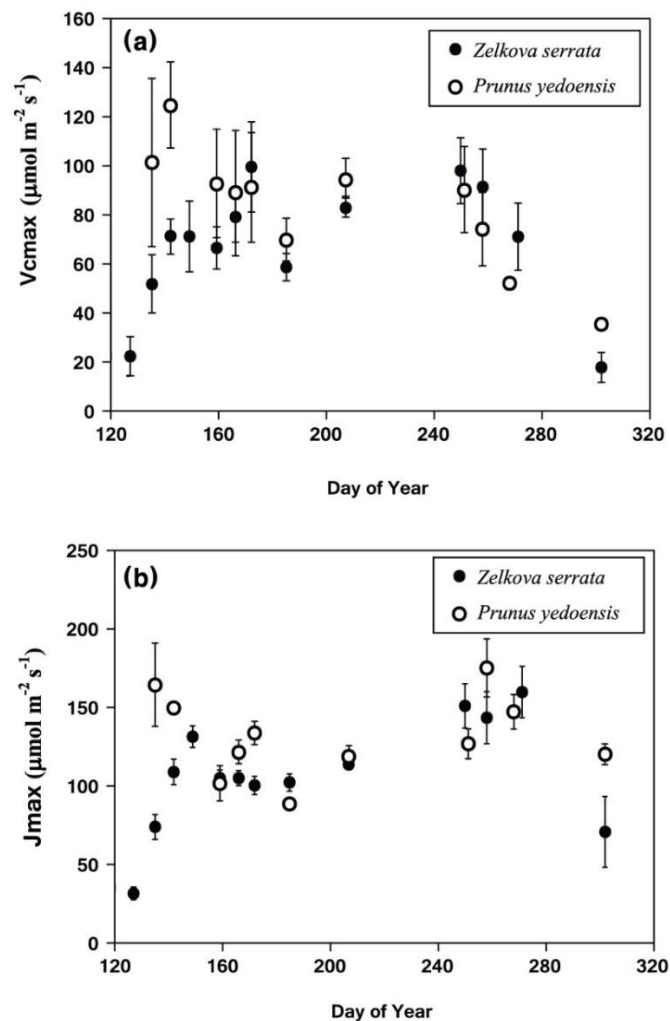


Fig. 2. Seasonal variation in (a) V_{cmax} and (b) J_{max} for *Zelkova serrata* and *Prunus yedoensis* Matsum. Error bars indicate 95% CI.

2. Can V_{cmax} and J_{max} be estimated indirectly from leaf traits data?

We confirmed the possibility of estimating the photosynthetic parameters from leaf N content per unit leaf area for data measured during the summer (DOY 207–255) across the species. These data showed significant correlations between V_{cmax} and J_{max} ($R = 0.85$, $P < 0.001$; Fig. 4), and between V_{cmax} and N content ($R = 0.7$, $P < 0.001$; Fig. 3). The slope of the linear relationship between V_{cmax} and J_{max} (0.76) was lower than those reported previously; i.e., 1.2–3.33 (Grassi et al., 2005; Wilson et al., 2000; Wullschleger, 1993).

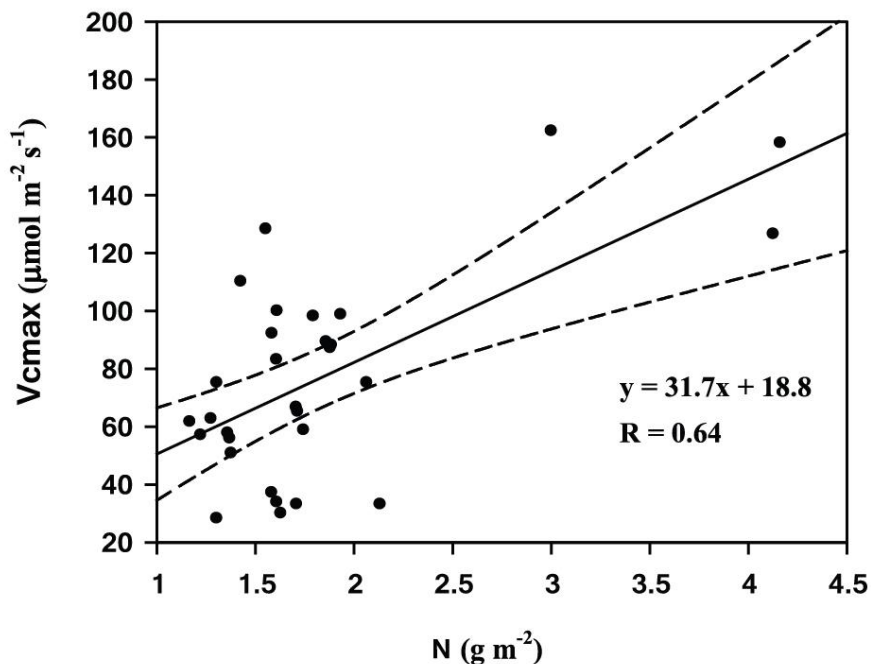


Fig. 3. Comparison of the leaf nitrogen content per unit area and V_{cmax} for 10 species measured during the peak growing season.

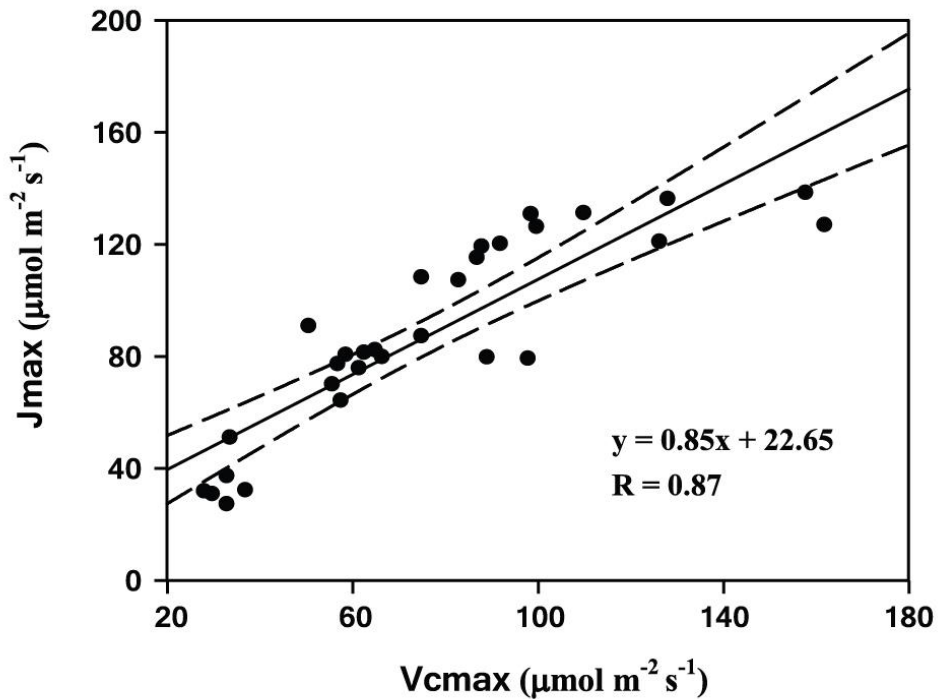


Fig. 4. Comparison of V_{cmax} and J_{max} for 10 species measured during the peak growing season.

However, we found no significant correlation between V_{cmax} and N content for the data on *Z. serrata* and *Pr. yedoensis* measured over the seasons ($R = 0.07$, $P = 0.16$). We speculate that the summer monsoon decouples the V_{cmax} and N relationship. The study year (2013) experienced a remarkably long monsoon period (DOY 168–216). We assume that both the low-light environment caused by frequent clouds and rainfall would decrease the leaf N content during the monsoon period (34 days of precipitation with 20 mm

day⁻¹ on average according to a weather station located 1 km from the study site; Korea Meteorological Administration). Continuous rainfall might have reduced leaf N contents because N leaching could account for ~15% of the total amount of N returned from the leaves to soils (Chapin and Moilanen, 1991; Lambers et al., 1998). Indeed, our results showed that leaf N contents in the two species decreased significantly during the monsoon period (shaded area in Fig. 5), whereas the V_{cmax} values of both species were fairly stable during that period (Fig. 2). Furthermore, during autumn, leaf N contents increased (Fig. 5), which is contrary to the nutrient resorption pattern (i.e., reduction of leaf N contents due to leaf nutrient withdrawal by plants before leaf abscission; Reich et al. 1991; Wilson et al. 2000). We do not have strong evidence for the uncommon pattern of leaf N seasonality at this study site. We speculate that a prolonged monsoon period and sufficient N input to the urban park through atmospheric N deposition and fertilization might be related to the leaf N seasonality.

We found a significant correlation between V_{cmax} and J_{max} for *Z. serrata* and *Pr. yedoensis* across the seasons ($R = 0.85$, $P < 0.01$). Thus, the tight correlations between V_{cmax} and J_{max} were valid both spatially during the peak growing season and temporally across seasons. Thus, finding correlations between leaf N contents and V_{cmax} is the essential step. Leaf N contents were predictive of V_{cmax} across 10 species during the peak growing season, but not

for the two species across the seasons. Identification of correlations between V_{cmax} and other variables—such as the LAI (Fig. 6)—over the seasons might offer an alternative method of inferring seasonality in V_{cmax} (Houborg et al., 2009; Ryu et al., 2011), although we were unable to test this hypothesis because the crowns from which the *Z. serrata* and *Pr. yedoensis* leaf samples were collected were not included in our LAI observation plots.

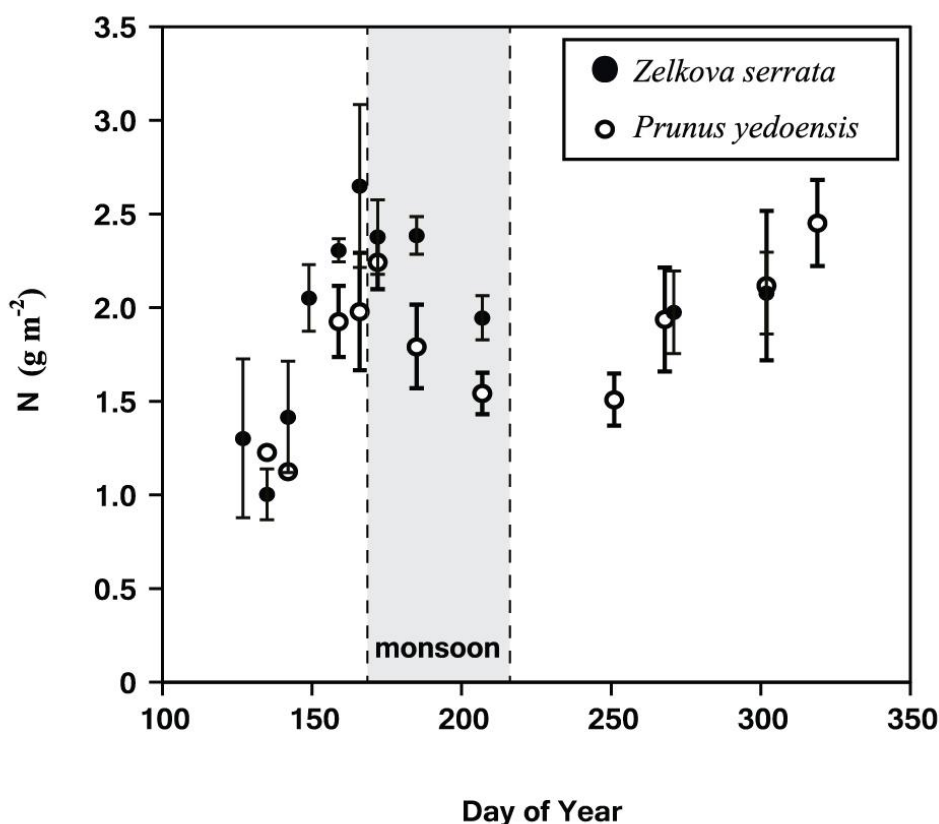


Fig. 5. Seasonal trend in leaf nitrogen content per unit area for *Zelkova serrata* and *Prunus yedoensis* Matsum. Error bars indicate 95% CI. The shaded area represents the monsoon period.

3. To what extent does the LAI vary across different land cover types over the seasons?

The peak LAI values derived from DCP varied from 3.1 to 4.4 across the plots in the park during the peak growing season (Fig. 6). All plots showed a clear seasonality in the LAI. We obtained the spatial distribution of the LAI for the entire park by merging in situ LAI observations using DCP and Landsat NDVI images (Fig. 7a). The LAI clearly showed considerable spatial variation from 1.03 to 3.76 at DOY 259.

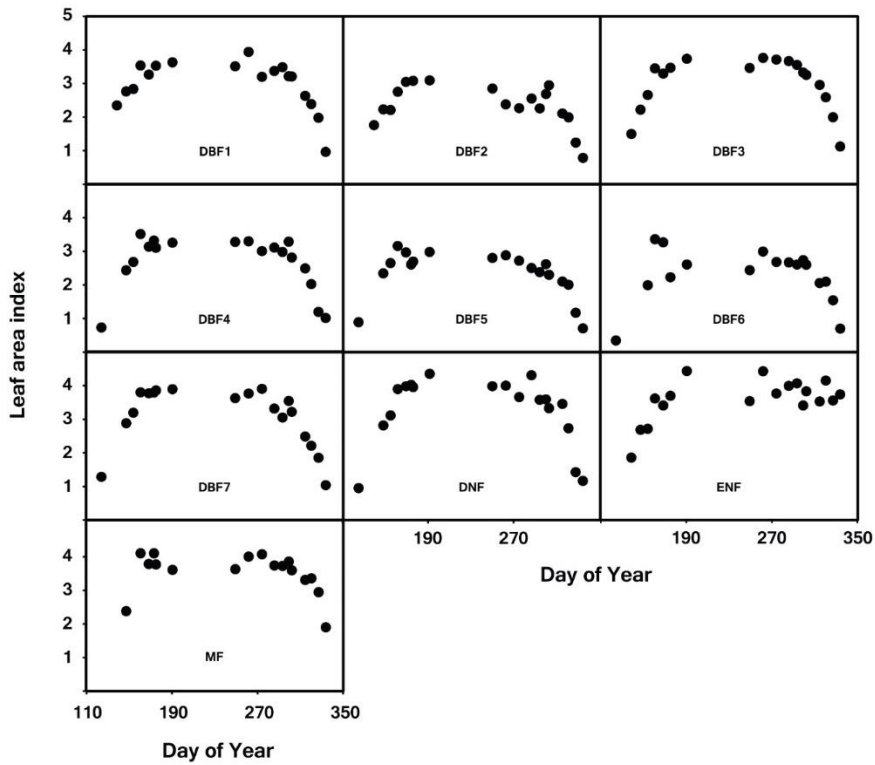


Fig. 6. Seasonal variation in the leaf area index in 10 plots.

We investigated the histograms of the LAI in the park for DOY 86, 131, 179, 259, and 355 (Fig. 7b). During winter, the histogram of the LAI showed the lowest mean \pm S.D. values (DOY 86: 0.97 ± 0.15 , DOY 355: 0.60 ± 0.13). The skewness and kurtosis were close to 0 and 3, respectively, indicating that the histograms followed a normal distribution. In the peak growing season (e.g., DOY 259), the LAI values showed the largest spread in distribution (0.55 S.D.) and a non-normal distribution caused by higher kurtosis (4.49), which was skewed left (-1.20). The non-normal, considerable spread in the LAI distribution reflects the heterogeneous canopy structure in the urban park, which cannot be represented by a single mean value.

Given the large spatial and temporal variations in photosynthetic parameters and LAI, we argue that individual tree-based 3D canopy photosynthesis models such as FLiES (Kobayashi and Iwabuchi, 2008) and MAESTRA (Wang and Jarvis, 1990) will be essential for predicting canopy photosynthesis in urban parks. We acknowledge that the 30-m resolution in Landsat images might be insufficient to capture spatial heterogeneity in urban parks. Recent advances in light detection and ranging (LiDAR) offers new opportunities to extract 3D canopy structure information, which will facilitate quantification of the complex canopy structures in urban parks.

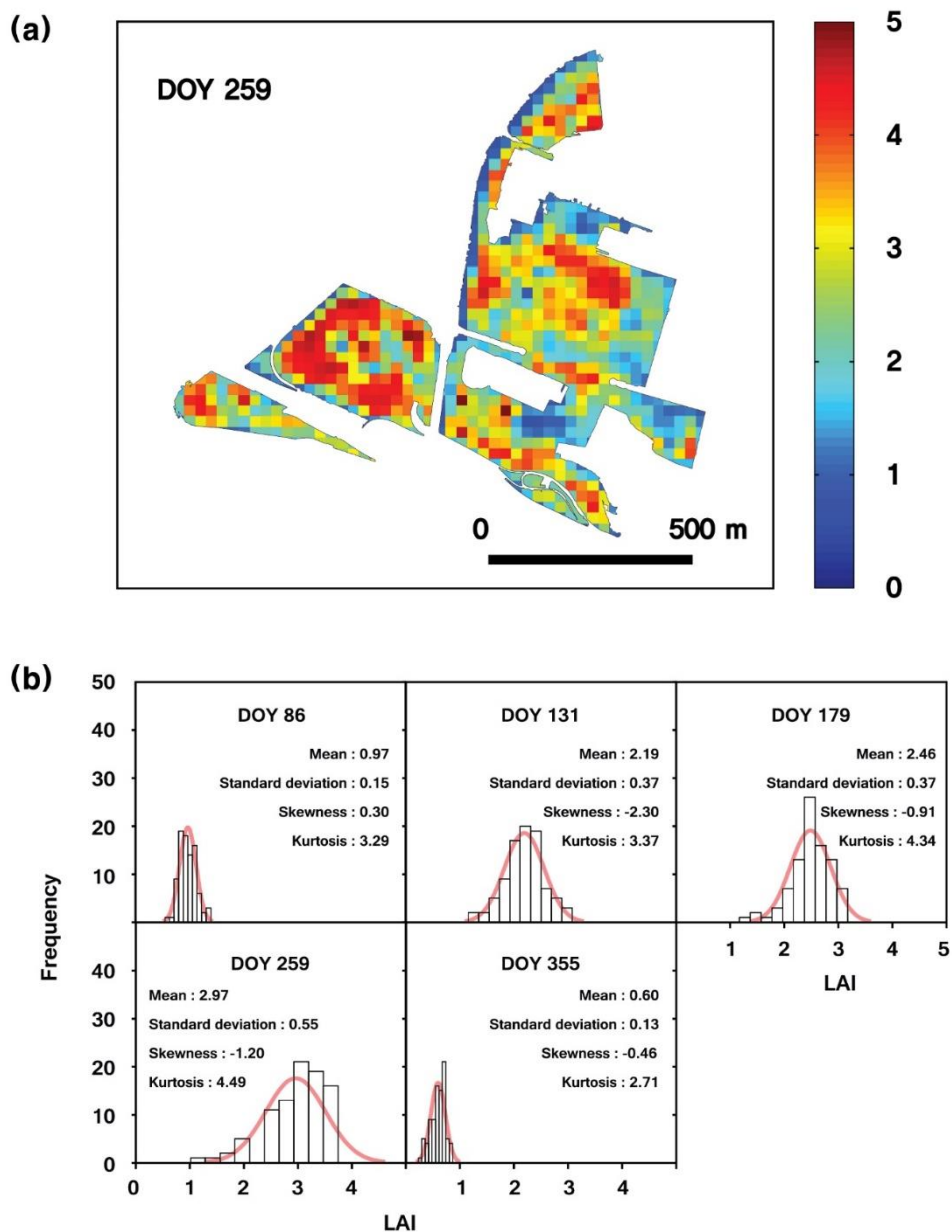


Fig. 7. (a) Leaf area index (LAI) map for day of year (DOY) 259 derived from Landsat images. (b) Histograms of Landsat-derived LAI values in the park for DOY 86, 131, 179, 259, and 355. The curves indicate histograms fit to a normal distribution.

4. Can park design strategy affect carbon and energy fluxes?

The model simulated carbon and energy fluxes were accurate compared to the eddy covariance measurement results (R squared values were 0.77, 0.76, 0.61 for latent- and sensible heat fluxes, and net ecosystem exchange, respectively; Fig. 9). Considering that the nighttime footprint of the flux measurement would expand beyond the canopies, thus to include roads with heavy traffic, mismatch between the simulation result and the measurement could be partially explained with carbon emission from the traffic. Negative anomalies in model simulated latent heat flux might be resulted from none of consideration of water surface although the simulated plot includes a small pond. This, in turn, caused positive anomalies in sensible heat flux with energy balance algorithm (Kyaw Tha Paw, 1987).

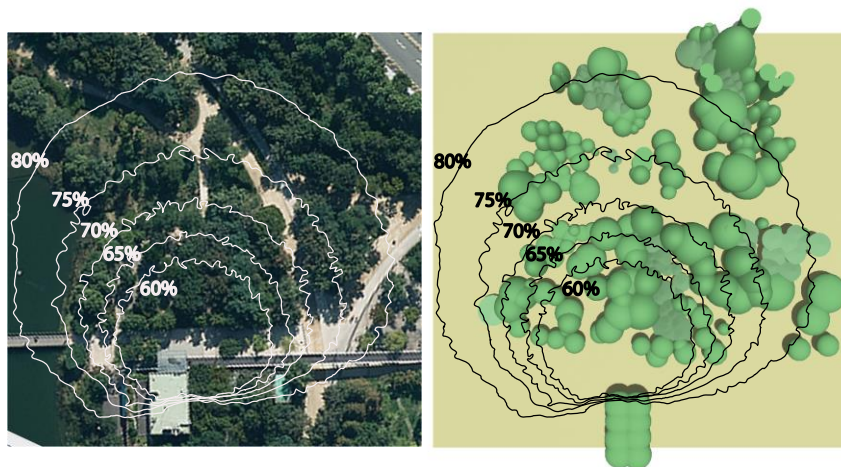


Fig. 8. Satellite image (left), and visualized input data (right) of the model simulation plot site (120 m by 120 m). Circles in both plots represents the footprint of the eddy covariance measurement.

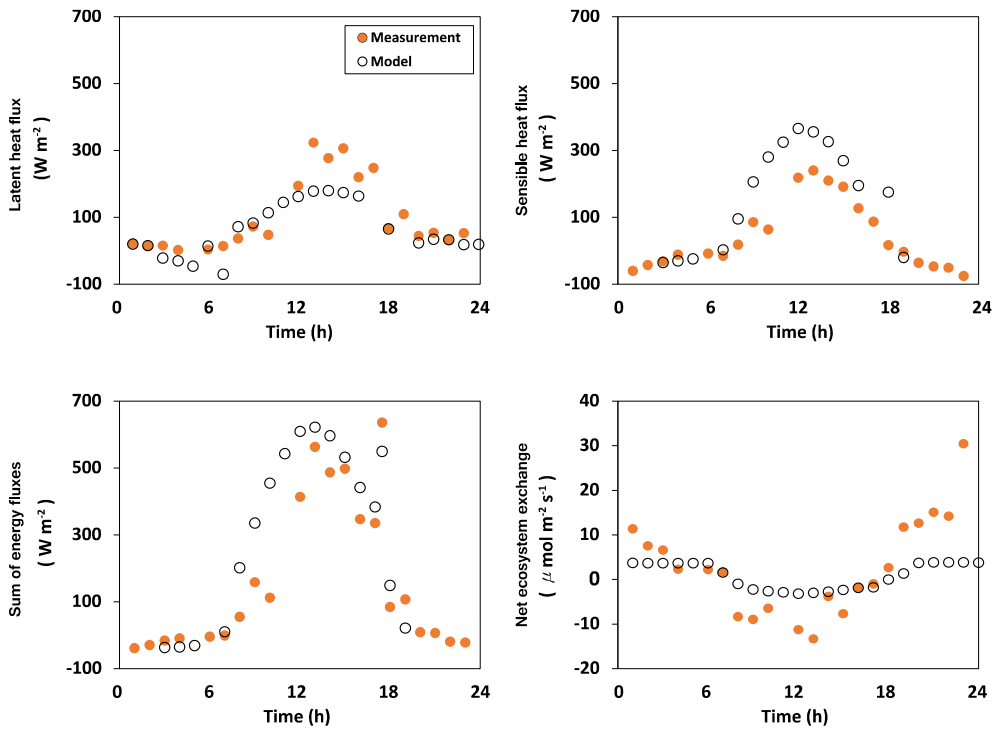


Fig. 9. Comparison between the simulated-, and measured carbon and energy fluxes in the plot. Extreme values with numerical errors are manually eliminated.

Under simplistic scenarios, the model simulated results showed that carbon and energy fluxes change with difference in park vegetation composition (Fig. 10, Fig. 11). Difference in tree distribution lead to little difference (less than 10 %) in both carbon and energy fluxes (Fig. 10), but difference in tree size significantly affected the results ($\sim 40\%$). We suspect the effect of the difference in crown cover of the scenarios with different tree sizes would have been dominant as higher crown cover largely affect absorbed radiation, which could lead to large difference in photosynthesis and energy partitioning. Contrasting results from the two sets of simulations clearly show what factor

is effective and what is not, even in this simplistic simulations.

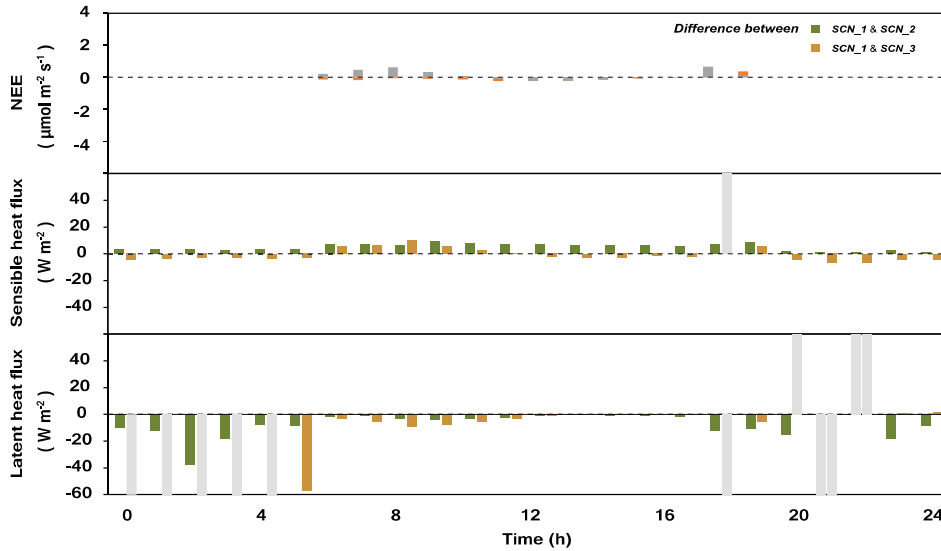


Fig. 10. Difference of results between SCN_1 and SCN_2, and SCN_1 and SCN_3. See Table 2 for scenarios in the legend.

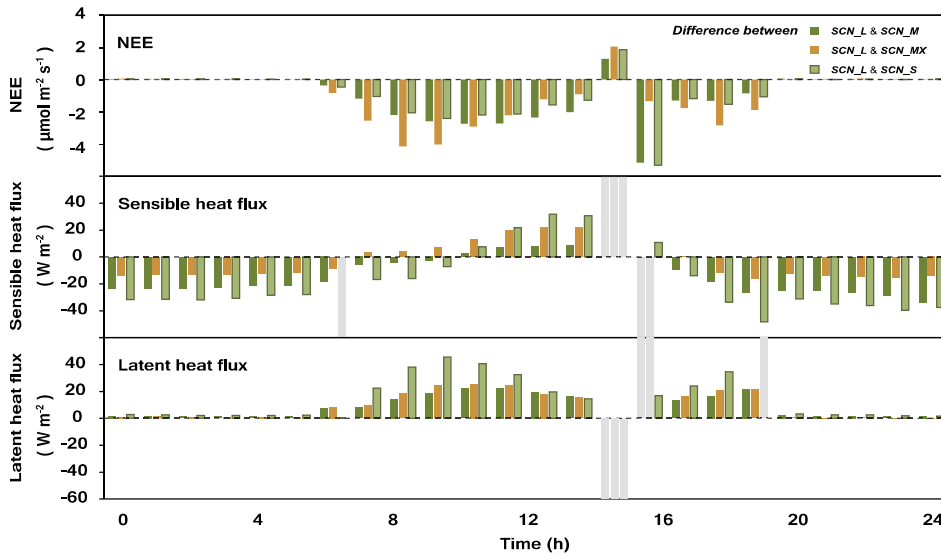


Fig. 11. Difference of results between SCN_L and SCN_M, SCN_L and SCN_MX, and SCN_L and SCN_S. See Table 2 for scenarios in the legend.

5. Broader implications for future urban park design

Urban planners and designers have paid less attention to the potential role in carbon uptake by plants. Mixture of open space and clumped canopy with diverse species, which promotes diverse activities by visitors, pervades in many urban parks. As shown in the results, the study site included a range of different species with large spatial and temporal variability in canopy structure and photosynthetic parameters (Figure 1 and 7). Canopy photosynthesis generally increases with light when solar irradiance is low, and it becomes saturated when solar irradiance is high. Trees that have high V_{cmax} (i.e. a proxy of photosynthetic capacity) could increase canopy photosynthesis even in high solar radiation conditions. Thus, archiving V_{cmax} values in typical urban park tree species will be useful in selecting tree species in planting design. For example, in isolated, sparsely distributed, or row-planted canopies, planting trees with higher V_{cmax} which could more efficiently use high level of solar irradiance would be desirable to enhance canopy photosynthesis. We do not argue carbon capture is the most important function in urban parks; rather, we hope carbon sequestration could be harmonized in the ecosystem services that urban parks provide. Owing to 3D canopy photosynthesis models, it is possible to simulate carbon fluxes with a range of different scenarios that include different plant distributions, plant species, canopy heights and multi-layered canopy structures. We expect

further applications of 3D canopy photosynthesis model into urban parks will be warranted in the future studies to better understand carbon cycles in urban regions as well as to help simulation-informed park planning and design.

IV. Summary and conclusions

In this report, we described the spatial and temporal patterns in photosynthetic parameters (V_{cmax} and J_{max}) and the LAI in an urban park in Seoul. The answers to the three scientific questions are as follows: (1) To what extent do photosynthetic parameters vary spatially during the peak growing season and temporally across the seasons? During the peak growing season, we found an eightfold difference in V_{cmax} and fourfold difference in J_{max} across 10 species. Over the seasons, two woody species (*Z. serrata* and *Pr. yedoensis*) showed three- to fivefold differences in V_{cmax} and two- to fivefold differences in J_{max} , respectively. (2) Can one estimate V_{cmax} and J_{max} indirectly from leaf traits data? We found that the leaf N content was predictive of V_{cmax} across 10 species during the peak growing season. Also, a strong positive correlation existed between V_{cmax} and J_{max} . However, across the seasons, the leaf N content was not significantly correlated with V_{cmax} , probably because of the prolonged summer monsoon. Thus, we did not find a universal relationship among leaf N, V_{cmax} , and J_{max} . (3) To what extent does the LAI vary across land cover types over the seasons? LAI maps derived from the Landsat NDVI and in situ LAI observations revealed a normal distribution with a small spread in LAI values in winter, whereas a non-normal distribution with a large

spread in LAI estimates was observed during the peak growing season. (4) Can park design strategy affect carbon and energy fluxes? Model validation against the measurement proved reliable model performance, and further simulations revealed significant differences from different tree size, but not from different tree distribution implicating the model simulation could be used for evaluating park designs in terms of carbon and energy fluxes. Our findings highlight the possibilities of large spatial and temporal variation in photosynthesis, and the potential effects of park designs on carbon and energy fluxes in urban parks. Thus, we conclude that the use of an individual-tree-based, 3D canopy photosynthesis model is essential for accurately predicting canopy photosynthesis, and is capable of evaluating park designs in terms of carbon budget and energy partitioning.

Reference

- Amthor, J., 1994: Scaling co₂-photosynthesis relationships from the leaf to the canopy. *Photosynthesis Research*, 39, 321-350
- Angel, S., Parent, J., Civco, D.L., Blei, A., & Potere, D., 2011: The dimensions of global urban expansion: Estimates and projections for all countries, 2000-2050. *Progress in Planning*, 75, 53-107
- Bae, J., & Ryu, Y., 2014: Large spatial and temporal variations of the soil organic carbon stocks in a constructed urban park. *Landscape and Urban Planning*
- Baldocchi, D., 1997: Measuring and modelling carbon dioxide and water vapour exchange over a temperate broad-leaved forest during the 1995 summer drought. *Plant Cell and Environment*, 20, 1108-1122
- Baldocchi, D.D., Xu, L., & Kiang, N., 2004: How plant functional-type, weather, seasonal drought, and soil physical properties alter water and energy fluxes of an oak–grass savanna and an annual grassland. *Agricultural and Forest Meteorology*, 123, 13-39
- Beer, C., Reichstein, M., Tomelleri, E., Ciais, P., Jung, M., Carvalhais, N., Rodenbeck, C., Arain, M.A., Baldocchi, D., Bonan, G.B., Bondeau, A., Cescatti, A., Lasslop, G., Lindroth, A., Lomas, M., Luysaert, S., Margolis, H., Oleson, K.W., Rouspard, O., Veenendaal, E., Viovy, N., Williams, C., Woodward, F.I., & Papale, D., 2010: Terrestrial gross carbon dioxide uptake: Global distribution and covariation with climate. *Science*, 329, 834-838
- Birol, F., Morgan, T., Cozzi, L., Emoto, H., Argiri, M., Rech, O., Malyshev, T., Bennaceur, K., Centurelli, R., Chen, M.-X., Dowling, P., Lyons, L., Magne, B., Mullin, C., Ocal, U., Olejarnik, P., Roques, F., Sassi, O., Sims, R., & Mooney, S. (2008). *World energy outlook 2008*. OECD Publishing

- Cao, X., Onishi, A., Chen, J., & Imura, H., 2010: Quantifying the cool island intensity of urban parks using aster and ikonos data. *Landscape and Urban Planning*, 96, 224-231
- Chapin, F.S., III, & Moilanen, L., 1991: Nutritional controls over nitrogen and phosphorus resorption from alaskan birch leaves. *Ecology*, 72, 709-715
- Chen, J.M., 1996: Optically-based methods for measuring seasonal variation of leaf area index in boreal conifer stands. *Agricultural and Forest Meteorology*, 80, 135-163
- Chiesura, A., 2004: The role of urban parks for the sustainable city. *Landscape and Urban Planning*, 68, 129-138
- dePury, D.G.G., & Farquhar, G.D., 1997: Simple scaling of photosynthesis from leaves to canopies without the errors of big-leaf models. *Plant Cell and Environment*, 20, 537-557
- Domingues, T.F., Martinelli, L.A., & Ehleringer, J.R., 2012: Seasonal patterns of leaf-level photosynthetic gas exchange in an eastern amazonian rain forest. *Plant Ecology & Diversity*, 7, 189-203
- Farquhar, G.D., Caemmerer, S.V., & Berry, J.A., 1980: A biochemical-model of photosynthetic co₂ assimilation in leaves of c-3 species. *Planta*, 149, 78-90
- Friend, A.D., 1995: Pgen: An integrated model of leaf photosynthesis, transpiration, and conductance. *Ecological Modelling*, 77, 233-255
- Gower, S.T., & Norman, J.M., 1991: Rapid estimation of leaf-area index in conifer and broad-leaf plantations. *Ecology*, 72, 1896-1900
- Grassi, G., Vicinelli, E., Ponti, F., Cantoni, L., & Magnani, F., 2005: Seasonal and interannual variability of photosynthetic capacity in relation to leaf nitrogen in a deciduous forest plantation in northern italy. *Tree Physiology*, 25, 349-360

- Houborg, R., Anderson, M.C., Norman, J.M., Wilson, T., & Meyers, T., 2009: Intercomparison of a 'bottom-up' and 'top-down' modeling paradigm for estimating carbon and energy fluxes over a variety of vegetative regimes across the us. *Agricultural and Forest Meteorology*, 149, 1875-1895
- Hutyra, L.R., Yoon, B., & Alberti, M., 2011: Terrestrial carbon stocks across a gradient of urbanization: A study of the seattle, wa region. *Global Change Biology*, 17, 783-797
- IEA (2013). *Co2 emissions from fuel combustion 2013*. OECD Publishing
- Jim, C.Y., & Chen, W.Y., 2006: Recreation–amenity use and contingent valuation of urban greenspaces in guangzhou, china. *Landscape and Urban Planning*, 75, 81-96
- Kattge, J., Knorr, W., Raddatz, T., & Wirth, C., 2009: Quantifying photosynthetic capacity and its relationship to leaf nitrogen content for global-scale terrestrial biosphere models. *Global Change Biology*, 15, 976-991
- Kobayashi, H., & Iwabuchi, H., 2008: A coupled 1-d atmosphere and 3-d canopy radiative transfer model for canopy reflectance, light environment, and photosynthesis simulation in a heterogeneous landscape. *Remote Sensing of Environment*, 112, 173-185
- Kyaw Tha Paw, U., 1987: Mathematical analysis of the operative temperature and energy budget. *Journal of Thermal Biology*, 12, 227-233
- Lambers, H., Chapin, F.S., III, & Pons, T., L (1998). *Plant physiological ecology*. Springer
- Leuning, R., Kelliher, F.M., Depury, D.G.G., & Schulze, E.D., 1995: Leaf nitrogen, photosynthesis, conductance and transpiration - scaling from leaves to canopies. *Plant Cell and Environment*, 18, 1183-1200

- Macfarlane, C., 2011: Classification method of mixed pixels does not affect canopy metrics from digital images of forest overstorey. *Agricultural and Forest Meteorology*, 151, 833-840
- Macfarlane, C., Hoffman, M., Eamus, D., Kerp, N., Higginson, S., McMurtrie, R., & Adams, M., 2007: Estimation of leaf area index in eucalypt forest using digital photography. *Agricultural and Forest Meteorology*, 143, 176-188
- Medlyn, B.E., Badeck, F.W., De Pury, D.G.G., Barton, C.V.M., Broadmeadow, M., Ceulemans, R., De Angelis, P., Forstreuter, M., Jach, M.E., Kellomaki, S., Laitat, E., Marek, M., Philippot, S., Rey, A., Strassmeyer, J., Laitinen, K., Liozon, R., Portier, B., Roberntz, P., Wang, K., & Jarvis, P.G., 1999: Effects of elevated co2 on photosynthesis in european forest species: A meta-analysis of model parameters. *Plant Cell and Environment*, 22, 1475-1495
- Millward, A.A., & Sabir, S., 2010: Structure of a forested urban park: Implications for strategic management. *Journal of Environmental Management*, 91, 2215-2224
- Muraoka, H., Saigusa, N., Nasahara, K.N., Noda, H., Yoshino, J., Saitoh, T.M., Nagai, S., Murayama, S., & Koizumi, H., 2010: Effects of seasonal and interannual variations in leaf photosynthesis and canopy leaf area index on gross primary production of a cool-temperate deciduous broadleaf forest in takayama, japan. *Journal of Plant Research*, 123, 563-576
- Myneni, R.B., Hoffman, S., Knyazikhin, Y., Privette, J.L., Glassy, J., Tian, Y., Wang, Y., Song, X., Zhang, Y., Smith, G.R., Lotsch, A., Friedl, M., Morisette, J.T., Votava, P., Nemani, R.R., & Running, S.W., 2002: Global products of vegetation leaf area and fraction absorbed par from year one of modis data. *Remote Sensing of Environment*, 83,

214-231

- Nilson, T., 1971: A theoretical analysis of the frequency of gaps in plant stands. *Agricultural Meteorology*, 8, 25-38
- Osnas, J.L.D., Lichstein, J.W., Reich, P.B., & Pacala, S.W., 2013: Global leaf trait relationships: Mass, area, and the leaf economics spectrum. *Science*, 340, 741-744
- Pentland, A.P., 1987: A new sense for depth of field. *Pattern Analysis and Machine Intelligence, IEEE Transactions on, PAMI-9*, 523-531
- Reich, P.B., Walters, M.B., & Ellsworth, D.S., 1991: Leaf age and season influence the relationships between leaf nitrogen, leaf mass per area and photosynthesis in maple and oak trees. *Plant Cell and Environment*, 14, 251-259
- Ryu, Y., Baldocchi, D.D., Kobayashi, H., van Ingen, C., Li, J., Black, T.A., Beringer, J., van Gorsel, E., Knohl, A., Law, B.E., & Rouspard, O., 2011: Integration of modis land and atmosphere products with a coupled-process model to estimate gross primary productivity and evapotranspiration from 1 km to global scales. *Global Biogeochemical Cycles*, 25, <http://dx.doi.org/10.1029/2011gb004053>
- Ryu, Y., Baldocchi, D.D., Verfaillie, J., Ma, S., Falk, M., Ruiz-Mercado, I., Hehn, T., & Sonnentag, O., 2010a: Testing the performance of a novel spectral reflectance sensor, built with light emitting diodes (leds), to monitor ecosystem metabolism, structure and function. *Agricultural and Forest Meteorology*, 150, 1597-1606
- Ryu, Y., Lee, G., Seon, S., Song, Y., & Kimm, H., 2014: Monitoring multi-layer canopy spring phenology of temperate deciduous and evergreen forests using low-cost spectral sensors. *Remote Sensing of Environment*, 149, 227-238

- Ryu, Y., Nilson, T., Kobayashi, H., Sonnentag, O., Law, B.E., & Baldocchi, D.D., 2010b: On the correct estimation of effective leaf area index: Does it reveal information on clumping effects? *Agricultural and Forest Meteorology*, 150, 463-472
- Ryu, Y., Sonnentag, O., Nilson, T., Vargas, R., Kobayashi, H., Wenk, R., & Baldocchi, D.D., 2010c: How to quantify tree leaf area index in an open savanna ecosystem: A multi-instrument and multi-model approach. *Agricultural and Forest Meteorology*, 150, 63-76
- Ryu, Y., Verfaillie, J., Macfarlane, C., Kobayashi, H., Sonnentag, O., Vargas, R., Ma, S., & Baldocchi, D.D., 2012: Continuous observation of tree leaf area index at ecosystem scale using upward-pointing digital cameras. *Remote Sensing of Environment*, 126, 116-125
- Sellers, P.J., Dickinson, R.E., Randall, D.A., Betts, A.K., Hall, F.G., Berry, J.A., Collatz, G.J., Denning, A.S., Mooney, H.A., Nobre, C.A., Sato, N., Field, C.B., & Henderson-Sellers, A., 1997: Modeling the exchanges of energy, water, and carbon between continents and the atmosphere. *Science*, 275, 502-509
- Seto, K.C., & Fragkias, M., 2005: Quantifying spatiotemporal patterns of urban land-use change in four cities of china with time series landscape metrics. *Landscape Ecology*, 20, 871-888
- Seto, K.C., Gueneralp, B., & Hutyrá, L.R., 2012: Global forecasts of urban expansion to 2030 and direct impacts on biodiversity and carbon pools. *Proceedings of the National Academy of Sciences of the United States of America*, 109, 16083-16088
- Sharkey, T.D., Bernacchi, C.J., Farquhar, G.D., & Singaas, E.L., 2007: Fitting photosynthetic carbon dioxide response curves for c-3 leaves. *Plant Cell and Environment*, 30, 1035-1040
- Song, C., Woodcock, C.E., Seto, K.C., Lenney, M.P., & Macomber, S.A.,

- 2001: Classification and change detection using landsat tm data: When and how to correct atmospheric effects? *Remote Sensing of Environment*, 75, 230-244
- Thompson, C.W., 2002: Urban open space in the 21st century. *Landscape and Urban Planning*, 60, 59-72
- Thompson, W.A., Huang, L.K., & Kriedemann, P.E., 1992: Photosynthetic response to light and nutrients in sun-tolerant and shade-tolerant rain-forest trees .2. Leaf gas-exchange and component processes of photosynthesis. *Australian Journal of Plant Physiology*, 19, 19-42
- Tucker, C.J., 1979: Red and photographic infrared linear combinations for monitoring vegetation. *Remote Sensing of Environment*, 8, 127-150
- Wang, Q., Iio, A., Tenhunen, J., & Kakubari, Y., 2008: Annual and seasonal variations in photosynthetic capacity of fagus crenata along an elevation gradient in the naeba mountains, japan. *Tree Physiology*, 28, 277-285
- Wang, Y.P., & Jarvis, P.G., 1990: Description and validation of an array model - maestro. *Agricultural and Forest Meteorology*, 51, 257-280
- Wilson, J.W., 1960: Inclined point quadrats. *New Phytologist*, 59, 1-7
- Wilson, K.B., Baldocchi, D.D., & Hanson, P.J., 2000: Spatial and seasonal variability of photosynthetic parameters and their relationship to leaf nitrogen in a deciduous forest. *Tree Physiology*, 20, 565-578
- Wright, I.J., Reich, P.B., Westoby, M., Ackerly, D.D., Baruch, Z., Bongers, F., Cavender-Bares, J., Chapin, T., Cornelissen, J.H.C., Diemer, M., Flexas, J., Garnier, E., Groom, P.K., Gulias, J., Hikosaka, K., Lamont, B.B., Lee, T., Lee, W., Lusk, C., Midgley, J.J., Navas, M.L., Niinemets, U., Oleksyn, J., Osada, N., Poorter, H., Poot, P., Prior, L., Pyankov, V.I., Roumet, C., Thomas, S.C., Tjoelker, M.G., Veneklaas, E.J., & Villar, R., 2004: The worldwide leaf economics

spectrum. *Nature*, 428, 821-827

Wullschleger, S.D., 1993: Biochemical limitations to carbon assimilation in c(3) plants - a retrospective analysis of the a/ci curves from 109 species. *Journal of Experimental Botany*, 44, 907-920

국문 초록

도시 공원은 도시 지역 내에서의 상당한 비율을 차지하지만, 기존의 도시 관련 연구들은 도시 공원 식생의 탄소 흡수에 대해서는 연구가 많이 이뤄지지 않았다. 일반적인 도시 공원은 다양한 수종을 포괄하고, 개방적 수관부의 배치를 통해 시간적, 공간적으로 매우 복잡한 경관을 구성한다. 따라서, 도시 공원에서의 광합성을 보다 잘 이해하기 위해서는 광합성 매개변수와 수관 구조 변수의 공간적, 시간적 차이를 관측하는 것이 필수적이다. 본 연구에서는 서울 숲 공원을 대상으로, 두 개의 핵심적인 광합성 매개변수 (최대 카르복시화율과 최대 전자 전달률을 나타내는 V_{cmax} 와 J_{max}) 와 엽면적지수의 계절적, 공간적 차이를 보인다. 최대 성장 시기에 10개의 수종 간에 V_{cmax} 와 J_{max} 는 각각 8배, 4배의 차이를 보였다. 계절적으로는 두 대표 수종인, 느티나무와 뽕나무가 V_{cmax} 에서는 각각 3배, 5배의 차이를, J_{max} 에서는 2배, 5배의 차이를 보였다. 본 연구는 또한 잎의 질소 함량을 통해 두 매개변수 추정 가능성이 가능한지를 평가했고, 최대 성장기의 10개 수종 대상의 관측자료에서는 질소 함량과 두 매개변수 사이에서의 상당한 상관관계를 확인했으나, 두 수종의 여러 계절 간 관측자료를 분석한 결과에서는 상관관계를 특정 지을 수 없었다. 엽면적 지수는 현장 관측과 위성 원격 탐사 영상을 통해 계산했으며, 시간적, 공간적으로 비정규분포를 보이며 큰 차이를 나타냈다. 정교하게 도시 공원 내 복잡한 구조적 특성을 반영한 3차원 모델은 탄소와 에너지 플럭스를 비교적 정확히 추정했다. 또한, 가상 시나리오를 활용한 모델 시뮬레이션은 수목의 분포와 개별 수관의 크기에 따른 효과를 명확히

보여주었다. 수목 분포 차이는 탄소 및 에너지 플럭스 결과에서 최대 3%의 차이만을 보였고, 반면에 개별 수관의 크기 차이는 최대 40%의 큰 차이를 보였다. 본 결과는 각각의 요소가 탄소수지 및 에너지 분할에 미칠 수 있는 효과를 평가할 수 있는 도구임을 시사한다. 위에서 제시된 본 논문의 결과들은 정확한 광합성 추정을 위해 광합성 매개변수 및 엽면적 지수의 공간적, 시간적 변이를 고려함이 중요함을 부각시킬 뿐 아니라, 공원 설계안 평가 플랫폼으로서의 3차원 모델링의 잠재적 역할을 시사한다.

주요어: 엽면적지수, 최대 카르복시화율, 최대 전자 전달률, 광합성, 3차원 모델링, 도시공원

학번: 2013-21147